ELSEVIER

Journal of Organometallic Chemistry 577 (1999) 323–329

Journal of Organometallic Chemistry

Syntheses and molecular structures of heterometallic carbonyl clusters derived from the triruthenium carbonyl methoxynitrido cluster; crystal and molecular structures of $[Ru_2Mo(\mu\text{-}H)(CO)_8(\eta^5\text{-}C_5H_5)(\mu_3\text{-}NOMe)]$, $[Ru_2Mo(\mu\text{-}H)(CO)_8(\eta^5\text{-}C_5H_5)(\mu_3\text{-}NH)]$ and $[Ru_3(CO)_{10}(\mu\text{-}NH_2)(\mu_3\text{-}Hg)\{Mo(\eta^5\text{-}C_5H_5)(CO)_3\}]$

Kenneth Ka-Hong Lee, Wing-Tak Wong *

Department of Chemistry, The University of Hong Kong, Pokfulam Road, Hong Kong, China

Received 9 September 1998

Abstract

Reaction of $[Ru_3(CO)_9(\mu_3\text{-}CO)(\mu_3\text{-}NOMe)]$ **1** with stoichiometric amounts of the hydrido complex $[(\eta^5\text{-}C_5H_5)Mo(CO)_3H]$ in THF at room temperature (r.t.) for 3 days affords the isolation of two new heterometallic trinuclear clusters namely $[Ru_2Mo(\mu\text{-}H)(CO)_8(\eta^5\text{-}C_5H_5)(\mu_3\text{-}NOMe)]$ **2** and $[Ru_2Mo(\mu\text{-}H)(CO)_8(\eta^5\text{-}C_5H_5)(\mu_3\text{-}NH)]$ **3** which both consist of a triangular Ru_2Mo core capped by a NR fragment (**2**: R = OMe; **3**: R = H). However, the reaction of **1** with the organomercurial derivative $[\{(\eta^5\text{-}C_5H_5)Mo(CO)_3\}_2Hg]$ resulted in the formation of a pentanuclear complex $[Ru_3(CO)_{10}(\mu\text{-}NH_2)(\mu_3\text{-}Hg)\{Mo(\eta^5\text{-}C_5H_5)(CO)_3\}]$ **4** in which a $(\eta^5\text{-}C_5H_5)Mo(CO)_3Hg$ fragment bridges the Ru_3 core on the opposite side of the amido group.

Keywords: Ruthenium; Molybdenum; Cluster; Methoxynitrido; Nitrene

1. Introduction

Mixed-metal clusters have received considerable attention and have become one of the popular research topics in cluster chemistry over the past decade. The Group VIII transition metal carbonyl clusters, such as ruthenium and osmium, are important elements in these heterometallic systems because of their good balance of reactivity and stability. In most of the cases, the building up of these heterometallic cluster species is aided by the presence of some main group non-metallic atoms such as carbon, nitrogen, oxygen, sulphur or phosphorus [1].

The chemistry of the triruthenium carbonyl methoxynitrido clusters such as $[Ru_3(CO)_9(\mu_3\text{-}CO)(\mu_3\text{-}NOMe)]$ has been described in previous papers by ourselves and others [2–4]. It was discovered that the reactivities of this class of methoxynitrido clusters originated from the thermolytic N–O bond cleavage to give either the nitrido or nitrene species such as the tetranuclear $[Ru_4(CO)_{12}(\mu_4\text{-}N)(\mu\text{-}OMe)]$ and hexanuclear $[Ru_6(CO)_{16}(\mu\text{-}CO)_2(\mu_4\text{-}NH)(\mu\text{-}OMe)_2]$ clusters [5]. In these reactions, cluster expansion is always accompanied with the N–O bond cleavage. It was also shown that the presence of additional cluster species such as $[Ru_3(CO)_{12}]$ during the hydrogenation of the methoxynitrido cluster $[Ru_3(CO)_9(\mu_3\text{-}CO)(\mu_3\text{-}NOMe)]$ resulted in the isolation of two higher nuclearity products $[Ru_5(\mu\text{-}H)_3(CO)_{13}(\mu_4\text{-}NH)(\mu_3\text{-}OMe)]$ and $[Ru_6(\mu\text{-}H)(CO)_{16}(\mu\text{-}CO)_2(\mu_4\text{-}NH)(\mu\text{-}OMe)]$ in addition to the two trinuclear species, $[Ru_3(\mu\text{-}H)_2(CO)_9(\mu_3\text{-}NOMe)]$ and $[Ru_3(\mu\text{-}H)_2(CO)_9(\mu_3\text{-}NH)]$ [5]. To generate some nitrido or nitrene clusters [6] utilising the methoxyni-

* Corresponding author. Tel.: +852-2547-2933.
E-mail address: wtwong@hkucc.hku.hk (W.-T. Wong)

0022-328X/99/$ - see front matter
PII: S0022-328X(98)01092-4

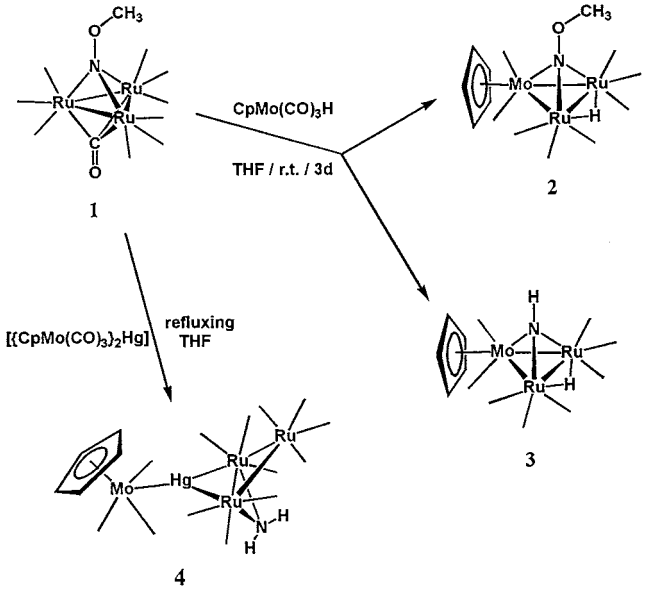

Scheme 1.

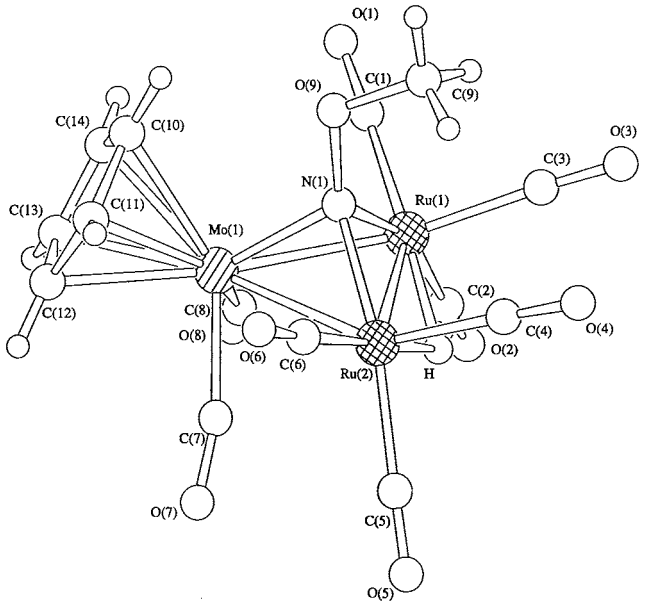

Fig. 1. The molecular structure of $[Ru_2Mo(\mu\text{-}H)(CO)_8(\eta^5\text{-}C_5H_5)(\mu_3\text{-}NOMe)]$ **2** with the atomic numbering scheme.

trido cluster as the building block, attempts to incorporate an external organometallic fragment are desirable. This synthetic approach gives not only new clusters, but also allows us to investigate the underlying mechanisms of their formation which has not been studied in detail so far. Herein, the reactions between the methoxynitrido cluster $[Ru_3(CO)_9(\mu_3\text{-}CO)(\mu_3\text{-}NOMe)]$ and the organo-molybdenum compounds which are described afford two heterometallic trinuclear clusters $[Ru_2Mo(\mu\text{-}H)(CO)_8(\eta^5\text{-}C_5H_5)(\mu_3\text{-}NR)]$ where R = OMe and H.

2. Results and discussion

Treatment of the cluster $[Ru_3(CO)_9(\mu_3\text{-}CO)(\mu_3\text{-}NOMe)]$ **1** with 1 equivalent of $[(\eta^5\text{-}C_5H_5)Mo(CO)_3H]$ in THF at r.t. for 3 days gave $[Ru_2Mo(\mu\text{-}H)(CO)_8(\eta^5\text{-}C_5H_5)(\mu_3\text{-}NOMe)]$ **2** and $[Ru_2Mo(\mu\text{-}H)(CO)_8(\eta^5\text{-}C_5H_5)(\mu_3\text{-}NH)]$ **3** in fair yields (Scheme 1) together with two known complexes, $[(\eta^5\text{-}C_5H_5)Mo(CO)_2]_2$ and $[(\eta^5\text{-}C_5H_5)Mo(CO)_3]_2$ [7] after TLC purification on silica. The spectroscopic data (IR, ^{1}H-NMR and FAB MS) for the two new clusters are summarised in Table 1. The ^{1}H-NMR and mass spectra of clusters **2** and **3** are fully consistent with their formulations. Single crystals of both **2** and **3**, suitable for X-ray diffraction analyses, were obtained by slow evaporation of their saturated *n*-hexane and dichloromethane solution mixtures at −20°C.

The molecular structure of **2** is illustrated in Fig. 1 and the selected bond lengths and angles are depicted in Table 2. The molecule contains a heterometallic Ru_2Mo triangular metal core [Ru(1)–Ru(2) 2.831(1), Ru(1)–Mo(1) 2.836(1) and Ru(2)–Mo(1) 2.834(1) Å] slightly asymmetrically capped by a methoxynitrido ligand through the coordination of nitrogen atom [Ru(1)–N(1) 2.025(7), Ru(2)–N(1) 2.014(7) and Mo(1)–N(1) 2.075(7) Å]. The N–O bond length was found to be 1.435(9) Å comparable to the parent cluster **1** [1.433(6) Å] [2,3]. The molybdenum atom is coordinated by a cyclopentadienyl ring in a η^5-fashion in accordance with the observation of a singlet at 5.5 ppm in the

Table 1
Spectroscopic data for clusters **2**–**4**

Cluster	IR(υ_{CO})[a] (cm^{-1})	^{1}H-NMR[c] (ppm)	MS[d] (m/z)
2	2091w, 2072vs, 2026s, 2008s, 1883br, 1831br	5.55 [s, 5H, C_5H_5], 3.67 [s, 3H, OMe], −17.55 [s, 1H, Ru–H]	633 (633)
3	2093m, 2072vs, 2020vs, 1850w	6.05 [br, 1H, NH], 5.50 [s, 5H, C_5H_5], −17.79 [s, 1H, Ru–H]	603 (603)
4	[b]2091w, 2049vs, 2041sh, 2004s, 1993m, 1974w, 1869w	5.42 [s, 5H, C_5H_5], 3.34 [br, 1H, NH], 2.24 [br, 1H, NH]	1045 (1045)

[a] Recorded in *n*-hexane.
[b] Recorded in CH_2Cl_2.
[c] Recorded in $CDCl_3$.
[d] Calculated value in parentheses.

^{1}H-NMR spectrum. The remaining coordination site in the Mo centre is bonded to two carbonyl ligands which can be considered to be semi-bridging as evidenced from the deviation from linearity in the bond angles of Mo(1)–C(7)–O(7) 167.3(9) and Mo(1)–C(8)–O(8) 165.9(9)° as well as the relatively short separation of Ru(1)···C(8) and Ru(2)···C(7) equal to 2.679(8) and 2.698(5) Å, respectively. A similar observation was found in the analogous compound $[Ru_2W(\mu\text{-H})(\eta^5\text{-}C_5H_5)(CO)_6(\mu\text{-CO})_2(\mu_3\text{-NPh})]$ [8]. Solution IR spectrum of **2** also supports this argument as two carbonyl stretching bands at 1883 and 1831 cm^{-1} were observed. Each Ru atom was bonded to two equatorial and one axial terminal carbonyls while the hydrido ligand presumably bridges the Ru(1)–Ru(2) edge since the metal–metal bond distance is comparable to hydride-bridged Ru–Ru separations in $[Ru_3(\mu\text{-H})_2(CO)_9(\mu_3\text{-NOMe})]$ [2.824(2) Å] and $[Ru_3(\mu\text{-H})_2(CO)_9(\mu_3\text{-NH})]$ [2.818(1) Å] [5], and is significantly longer than that in **1** [2.755(1) Å]. The methoxy group exhibits a singlet proton resonance at δ 3.67 which is essentially similar to that of **1** (δ 3.46) and $[Ru_3(\mu\text{-H})_2(CO)_9(\mu_3\text{-NOMe})]$ (δ 3.46) but relatively upfield (δ 5.46) to that in the $[CpMnFe_2Cp'_2(\mu\text{-CO})_2(\mu\text{-NO})(\mu_3\text{-NOMe})]^+$ ($Cp' = MeC_5H_4$) cation [9].

The molecular structure of **3** is depicted in Fig. 2 and some selected structural parameters are presented in Table 2. The molecular geometry of **3** resembled **2** except that the methoxy group is replaced by proton. The molecule consists of a trinuclear heterometallic $Ru_2Mo(\mu_3\text{-NH})$ nitrene metal core. The three metal atoms form an equilateral triangle with Ru(1)–Ru(2) 2.831(1), Ru(1)–Mo(1) 2.824(1) and Ru(2)–Mo(1) 2.829(1) Å in which the nitrene, N–H fragment triply bridged the triangular plane [Ru(1)–N(1) 2.023(8), Ru(2)–N(1) 2.052(8) and Mo(1)–N(1) 2.051(8) Å] similar to the geometry of the central core in $[(\eta^5\text{-}C_5H_4Me)Mo(\mu_3\text{-NH})(\mu\text{-NO})(\mu\text{-CO})Fe_2(CO)_6]$ [10] and $[Fe_2Co(\mu_3\text{-NH})(CO)_9]$ [11]. The remaining coordinated ligands such as η^5-C_5H_5 ring, carbonyls and bridging hydride within the metal framework are arranged in a similar manner to **2** including the semi-bridging carbonyls [Mo(1)–C(7)–O(7) 163(1) and Mo(1)–C(8)–O(8) 164(1)°] between the two heterometallic Ru–Mo edges [Ru(1)–C(8) 2.576(3) and Ru(2)–C(7) 2.617(6) Å]. The ^{1}H-NMR properties of cluster **3** are very similar to **2** in respect of the cyclopentadienyl group (δ 5.50) and metal hydride (δ −17.79). The nitrene proton, on the other hand, is located at 6.05 ppm as a broad peak that is similar to many previously identified nitrene-containing clusters [4,5].

Table 2
Selected bond distances (Å) and angles (°) of clusters **2** and **3**, with the estimated S.D. in parentheses

Bond distances (Å)		
Ru(1)–Ru(2)	2.831(1)	2.831(1)
Ru(1)–Mo(1)	2.836(1)	2.824(1)
Ru(2)–Mo(1)	2.834(1)	2.829(1)
Ru(1)–N(1)	2.025(7)	2.023(8)
Ru(2)–N(1)	2.014(7)	2.052(8)
Mo(1)–N(1)	2.075(7)	2.051(8)
Ru(1)–H	1.72	1.86
Ru(2)–H	1.89	1.84
N(1)–O(9)	1.435(9)	–
O(9)–C(9)	1.40(1)	–
N(1)–H(1)	–	1.01
Ru–CO	1.92(1)–1.97(1)	1.86(1)–1.91(1)
Mo–CO	1.97(1)–1.98(1)	1.92(1)–1.94(1)
C–O (carbonyl)	1.10(1)–1.15(1)	1.14 (1)–1.18(1)
Bond angles (°)		
Ru(1)–Ru(2)–Mo(1)	60.08(3)	59.86(3)
Ru(2)–Ru(1)–Mo(1)	60.00(3)	60.04(3)
Ru(1)–Mo(1)–Ru(2)	59.91(3)	60.10(3)
Ru(1)–N(1)–Ru(2)	89.0(3)	88.0(3)
Ru(1)–N(1)–Mo(1)	87.5(3)	87.8(3)
Ru(2)–N(1)–Mo(1)	87.7(3)	87.2(3)
Ru(1)–Ru(2)–C(4)	99.6(3)	95.7(3)
Ru(1)–Ru(2)–C(5)	121.0(3)	119.9(3)
Ru(2)–Ru(1)–C(2)	120.9(3)	119.2(4)
Ru(2)–Ru(1)–C(3)	97.5(3)	97.4(4)

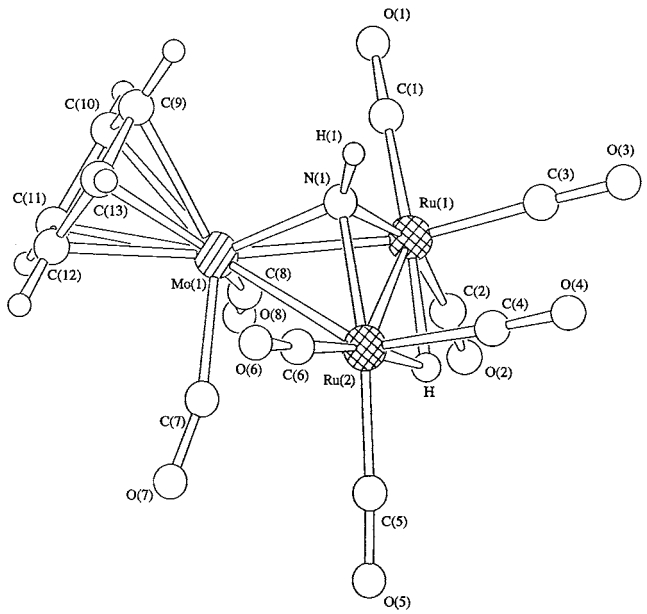

Fig. 2. The molecular structure of $[Ru_2Mo(\mu\text{-H})(CO)_8(\eta^5\text{-}C_5H_5)(\mu_3\text{-NH})]$ **3** with the atomic numbering scheme.

Although the conversion of methoxynitrido to nitrene moiety can be effected under an atmosphere of molecular hydrogen which has been demonstrated earlier from the hydrogenation of $[Ru_3(\mu\text{-H})_2(CO)_9(\mu_3\text{-NOMe})]$ to form $[Ru_3(\mu\text{-H})_2(CO)_9(\mu_3\text{-NH})]$, the isolation of both **2** and **3** is unexpected as one of the ruthenium vertex is replaced by an isoelectronic $(\eta^5\text{-}C_5H_5)Mo(CO)_2H$ fragment via a metal-exchange reaction rather than the incorporation of an extra heterometallic fragment to the triruthenium core. The

occurrence of metal-exchange reaction is known but not common in cluster reactions. The first example was reported in an attempt to generate an external Co–M bond by CO elimination through the thermolysis of $[Co_3(\mu_3\text{-}CR)(CO)_8AsMe_2MCo(CO)_3]$ which afforded instead of a tetranuclear complex, a trinuclear heterometallic cluster, $[CpMCo_2(\mu_3\text{-}CR)(CO)_8]$ (R = alkyl; M = Cr, Mo and W) [12]. On the other hand, Geoffory and co-workers have reported the formation of a heteronuclear nitrene cluster, $[Ru_2Co(\mu\text{-}H)(\mu_3\text{-}NPh)(CO)_9]$ via the metal-exchange reaction [13] between the nitrene cluster, $[Ru_3(CO)_9(\mu_3\text{-}CO)(\mu_3\text{-}NPh)]$ and $[Co(CO)_4]^-$ anion followed by protonation. Later, $[Ru_2W(\mu\text{-}H)(\eta^5\text{-}C_5H_5)(CO)_6(\mu\text{-}CO)_2(\mu_3\text{-}NPh)]$, the structural analogs of clusters **2** and **3**, were also isolated and characterized from the reaction of $[Ru_3(CO)_9(\mu_3\text{-}CO)(\mu_3\text{-}NPh)]$ with $[(\eta^5\text{-}C_5H_5)W(CO)_3H]$ [8]. Nonetheless, the mechanistic details for the formation of **2** and **3** remains uncertain as the metal-exchange reaction is an unpredictable and complicated process.

However, the reaction of an organometallic reagent which also possesses the $(\eta^5\text{-}C_5H_5)Mo(CO)_3$ fragment, such as $[\{(\eta^5\text{-}C_5H_5)Mo(CO)_3\}_2Hg]$ with **1** does not lead to the formation of clusters **2** and **3**. Reaction of a THF solution of cluster **1** with $[\{(\eta^5\text{-}C_5H_5)Mo(CO)_3\}_2Hg]$ in stoichiometric quantities at r.t. does not give an observable change while the reaction occurs at refluxing condition for 2 h and affords a new red heteronuclear cluster $[Ru_3(CO)_{10}(\mu\text{-}NH_2)(\mu_3\text{-}Hg)\{Mo(\eta^5\text{-}C_5H_5)(CO)_3\}]$ **4** as shown in Scheme 1. Cluster **4** has been fully characterised by IR, ^{1}H-NMR and MS with the spectroscopic data presented in Table 1. The positive FAB mass spectrum of **4** shows a parent envelope at m/z 1045 with an isotopic distribution consistent with the presence of three ruthenium, one molybdenum and one mercury atom. The IR spectrum shows the activities of terminal carbonyl. The occurrence of molybdenum is further supported by the appearance of a cyclopentadienyl ligand at δ 5.42. In addition, two broad peaks assigned to the bridging amido group were also noted in the ^{1}H-NMR spectrum of **4**.

In order to elucidate the structure of cluster **4**, red crystals of **4** were grown in a saturated solution mixture of *n*-hexane and dichloromethane after slow evaporation at −20°C. The molecular structure of **4**, established by X-ray diffraction analysis, is given in Fig. 3 and the bond parameters are tabulated in Table 3. The structure of **4** is comprised of a triangular $Ru_3(CO)_{10}(\mu\text{-}NH_2)$ core and a $(\eta^5\text{-}C_5H_5)Mo(CO)_3$ fragment bridged by a Hg atom in a μ_3-coordination mode similar to the metal skeleton of $[(\mu_3\text{-}\eta^2\text{-}C_2Bu^t)(CO)_9Ru_3(\mu_3\text{-}Hg)Mo(\eta^5\text{-}C_5H_5)(CO)_3]$ [14] and $[(\mu_3\text{-}H)(CO)_9Mn_3(\mu_3\text{-}Hg)Mo(\eta^5\text{-}C_5H_5)(CO)_3]$ [15]. The triruthenium core [Ru(1)–Ru(2) 2.831(1), Ru(1)–Ru(3) 2.836(1) and Ru(2)–Ru(3) 2.845(1) Å] is symmetrically bridged by an amido ligand with Ru(2)–N(1) and Ru(3)–N(1) of 2.111(7) and 2.084(8) Å, respectively. The Ru_3 core is bonded by ten terminal carbonyls [four for Ru(1), three for Ru(2) and Ru(3)] such that the geometry of this $Ru_3(CO)_{10}(\mu\text{-}NH_2)$ core is similar to that in $[Ru_3(\mu\text{-}H)(CO)_{10}(\mu\text{-}NH_2)]$ [16,17]. However, the Ru(2)–Ru(3) edge in $[Ru_3(\mu\text{-}H)(CO)_{10}(\mu\text{-}NH_2)]$ is bridged by a hydride ligand and with a relatively short [2.773(2) Å] distance in comparison to **4** [2.845(1) Å] which is bridged symmetrically by a $[Mo(\eta^5\text{-}C_5H_5)(CO)_3Hg]$ fragment with an average Hg–Ru distance of 2.793(8) Å. The Ru(2)–Hg(1)–Ru(3) angle is 61.24(2)° and is comparable to the value of 61.4(1)° found in $[(\mu_3\text{-}\eta^2\text{-}C_2Bu^t)(CO)_9Ru_3(\mu_3\text{-}Hg)Mo(\eta^5\text{-}C_5H_5)(CO)_3]$ [14]. The atom-defining planes Ru(2)–Hg(1)–Ru(3) and Ru(2)–N(1)–Ru(3) give dihedral angles of 124.4 and 113.8° with respect to the triruthenium plane, respectively. The Hg(1)–Mo(1)

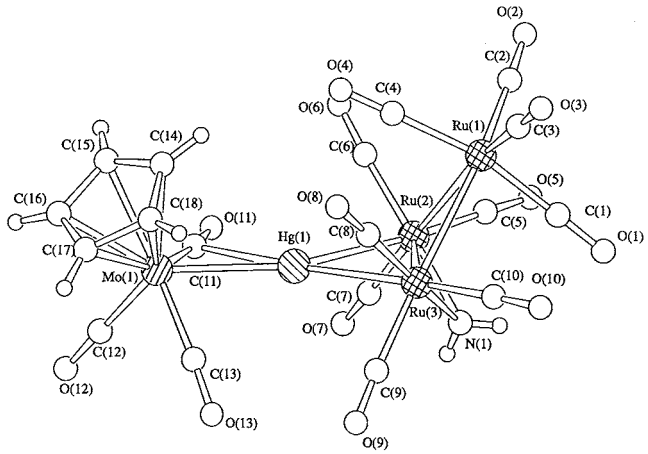

Fig. 3. The molecular structure of $[Ru_3(CO)_{10}(\mu\text{-}NH_2)(\mu_3\text{-}Hg)\{Mo(\eta^5\text{-}C_5H_5)(CO)_3\}]$ **4** with the atomic numbering scheme.

Table 3
Selected bond distances (Å) and angles (°) of cluster **4**, with the estimated S.D. in parentheses

Bond distances (Å)	
Ru(1)–Ru(2)	2.831(1)
Ru(2)–Ru(3)	2.845(1)
Ru(1)–Ru(3)	2.836(1)
Ru(2)–Hg(1)	2.8035(8)
Ru(3)–Hg(1)	2.7814(8)
Mo(1)–Hg(1)	2.7681(8)
Ru(2)–N(1)	2.111(7)
Ru(3)–N(1)	2.084(8)
Ru–CO	1.85(1)–1.94(1)
Mo–CO	1.944(10)–1.97(1)
C–O (carbonyl)	1.14(1)–1.18(1)
Bond angles (°)	
Ru(1)–Ru(2)–Ru(3)	59.96(3)
Ru(2)–Ru(1)–Ru(3)	60.26(3)
Ru(1)–Ru(3)–Ru(2)	59.78(3)
Ru(2)–Hg(1)–Ru(3)	61.24(2)
Ru(2)–Hg(1)–Mo(1)	148.54(3)
Ru(2)–N(1)–Ru(3)	85.4(3)

bond length in **4** [2.7681(8) Å] is longer than the corresponding separation in the dimeric starting complex, [{(η^5-C_5H_5)Mo(CO)$_3$}$_2$Hg] [2.685(3) Å] [18]. The orientation of the η^5-cyclopentadienyl moiety is pointed at the side of the Ru_3 plane opposite to the amido ligand since the non-bonded interactions are minimised with the two axial carbonyl groups [C(6)–O(6) and C(8)–O(8)] bonded to Ru(2) and Ru(3) atoms, respectively.

Although [{(η^5-C_5H_5)Mo(CO)$_3$}$_2$Hg] and [(η^5-C_5H_5)Mo(CO)$_3$H] possess the same isolobal (η^5-C_5H_5)Mo(CO)$_3$ fragment, the reaction with **1** afforded the new pentanuclear cluster **4** in addition to the known di-molybdenum complex. This external metal fragment only bridged across a Ru–Ru edge of a Ru_3 core similar to an isolobal metal–metal bridge hydride in [Ru_3(μ-H)(CO)$_{10}$(μ-NH$_2$)]. Moreover, the methoxynitrido ligand has been converted to an amido group other than the previously observed nitrido, nitrene or carbamate ligand. Nevertheless, the investigation of cluster building up ultilizing the methodology involving the methoxynitrido precursor is still in progress.

3. Experimental

3.1. General procedures

All manipulations were carried out under an inert atmosphere of argon with standard Schlenk technique, unless stated otherwise. Commercially available chemicals were used as received. Solvents were dried by appropriate drying agents and distilled prior to use. Preparative thin-layer chromatographic (TLC) plates were prepared from silica (Merck Kieselgel 60 GF_{254}). IR spectra were recorded on a Bio-rad FTS-165 FT-IR spectrometer using 0.5 mm CaF_2 solution cells. ^{1}H-NMR spectra were obtained on a Bruker DPX-300 NMR spectrometer using deuteriated solvents as lock and reference. Fast-atom bombardment (FAB) mass spectra were recorded on a Finnigan MAT 95 mass spectrometer. Elemental analyses were performed by the Butterworth Laboratories Ltd., UK.

3.2. Reaction of [$Ru_3(CO)_9(\mu_3$-CO)(μ_3-NOMe)] **1** with [(η^5-C_5H_5)Mo(CO)$_3$H]

Solids of **1** (125 mg, 0.2 mmol) and [(η^5-C_5H_5)Mo(CO)$_3$H] (49 mg, 0.2 mmol) were mixed and dried in vacuo for a few minutes. Then, 50 cm^3 of freshly distilled THF was added into the solid mixture. The yellow solution was stirred for 3 days with a colour change to orange. The solvent was removed under reduced pressure and the orange oily residue was chromatographed on silica gel plate. Elution with *n*-hexane/dichloromethane (4:1, v/v) yielded unreacted **1** (25 mg, 20%, R_f ca. 0.7), red [(η^5-C_5H_5)Mo(CO)$_2$]$_2$ (13 mg, 15%, R_f ca. 0.6) orange [(η^5-C_5H_5)Mo(CO)$_3$]$_2$ (10 mg, 10%, R_f ca. 0.5), orange [Ru_2Mo(μ-H)(CO)$_8$(η^5-C_5H_5)(μ_3-NOMe)] **2** (13 mg, 10%, R_f ca. 0.4) and orange [Ru_2Mo(μ-H)(CO)$_8$((η^5-C_5H_5)(μ_3-NH)] **3** (12 mg, 10%, R_f ca. 0.3).

3.3. Reaction of [$Ru_3(CO)_9(\mu_3$-CO)(μ_3-NOMe)] **1** with [{(η^5-C_5H_5)Mo(CO)$_3$}$_2$Hg]

A sample of **1** (125 mg, 0.2 mmol) and [{(η^5-C_5H_5)Mo(CO)$_3$}$_2$Hg] (138 mg, 0.2 mmol) were dissolved in 50 cm^3 of THF. The yellow solution was refluxed for 2 h to give a dark brown mixture. The solvent was then removed in vacuo and the residue was taken up in a minimum amount of CH_2Cl_2. Purification by preparative TLC using *n*-hexane/CH_2Cl_2 (3:1, v/v) yielded in order of elution, yellow [$Ru_3(CO)_{12}$] (7 mg, 5.5%, R_f ca. 0.8), unreacted **1** (10 mg, 8%, R_f ca. 0.6), orange [(η^5-C_5H_5)Mo(CO)$_3$]$_2$ (5 mg, 5%, R_f ca. 0.5) and orange–red [Ru_3(CO)$_{10}$(μ-NH$_2$)(μ_3-Hg){Mo(η^5-C_5H_5)-(CO)$_3$}] **4** (21 mg, 10%, R_f ca. 0.4).

4. X-Ray crystal structure determination

Single crystals of **2**–**4** for X-ray analyses were obtained as described above and mounted on top of a glass fiber by means of epoxy resin. Intensity data were collected on either a Rigaku-AFC7R or a MAR research image-plate scanner using graphite-monochromated Mo–K_α radiation ($\lambda = 0.71073$ Å) for unit-cell determination and data collection. A summary of the crystallographic data, structure solution and refinement is given in Table 4. The ω–2θ scan mode with a speed 16.0 deg min^{-1} was used for clusters **2** and **3**. For cluster **4**, 65 3° frames with an exposure time of 5 min per frame were used. Lorentz-polarisation and Ψ-scan absorption corrections [19] were applied to all the intensity data collected on a Rigaku-AFC7R diffractometer. However, an approximation to absorption correction by inter-image scaling was applied for **4**. Scattering factors were taken from Ref. ([20]a) and anomalous dispersion effects were included in Fc ([20]b). The positions of ruthenium atoms were determined by direct methods (SIR92) [21]. The remaining non-hydrogen atoms were determined by subsequent Fourier and difference Fourier techniques. The structures were refined by full-matrix least-squares analysis on F with all non-hydrogen atoms refined anisotropically until convergence was reached. The hydrides and hydrogen atoms of the nitrene and amido moieties were located by difference fourier synthesis using low angle data while hydrogen atoms of the organic moieties were generated in their ideal positions (C–H, 0.95 Å). They are included in the structure factors calculations but

Table 4
Summary of crystallographic parameters for clusters **2–4**

	2	**3**	**4**
Empirical formula	$C_{14}H_9NO_9Ru_2Mo$	$C_{13}H_7NO_8Ru_2Mo$	$C_{18}H_7NO_{13}Ru_3MoHg$
Formula weight	633.31	603.28	1044.99
Crystal system	Triclinic	Triclinic	Triclinic
Space group	$P\bar{1}$ (no. 2)	$P\bar{1}$ (no. 2)	$P\bar{1}$ (no. 2)
Unit cell dimensions			
a (Å)	8.627(1)	9.165(1)	8.334(1)
b (Å)	14.894(2)	16.012(2)	9.579(1)
c (Å)	7.372(1)	6.2907(9)	17.387(2)
α (°)	96.58(1)	95.98(1)	89.59(2)
β (°)	98.55(1)	108.90(1)	83.19(2)
γ (°)	88.64(1)	91.30(1)	69.75(2)
V (Å^3)	930.4(2)	867.0(2)	1292.2(3)
Z	2	2	2
$D_{calc.}$ (g cm^{-3})	2.260	2.311	2.686
$F(000)$	604	572	960
μ(Mo–K$_\alpha$)	23.12	24.71	81.84
Diffractometer	Rigaku-AFC7R	Rigaku-AFC7R	MAR research Image Plate Scanner
2θ range (°)	45	45	–
Scan type	ω–2θ	ω–2θ	–
Scan speed (in ω) (deg min^{-1})	16.0	16.0	–
Scan width (°)	$0.68+0.35\tan\theta$	$1.68+0.35\tan\theta$	–
No. of reflections measured	2617	2435	28878
No. of unique reflections	2425	2261	4430
No. of reflections with $I>3\sigma(I)$	2080	1734	3411
No. of variables	244	141	204
R[a]	0.034	0.039	0.039
R_w[b]	0.045	0.039	0.048
Goodness-of-fit	2.28	2.43	1.41
Largest Δ/σ	0.07	0.03	0.06
Residual electron density (e^{-3})	0.44 to −0.79	0.91 to −0.66	1.29 to −1.52

[a] $R=\Sigma\|\|F_o\|-\|F_c\|\|/\Sigma|F_o|$.
[b] $R_w=[\Sigma w(|F_o|-|F_c|)^2/\Sigma w(F_o)^2]^{1/2}$ where $w=[\sigma^2(F_o)]^{-1}$.

were not refined. All calculations were performed on a Silicon-Graphics computer using the program package TEXSAN [22].

Atomic coordinates, thermal parameters, and bond lengths and angles have been deposited at the Cambridge Crystallographic Data Centre (CCDC).

Acknowledgements

W.-T. Wong acknowledges financial support from the Hong Kong Research Grants Council and the University of Hong Kong. K.K.-H. Lee acknowledges the receipt of a postgraduate studentship, administered by the University of Hong Kong.

References

[1] D. Michael, P. Mingos, D.J. Wales, Introduction to Cluster Chemistry, Prentice Hall, Englewood Cliffs, NJ, 1990.
[2] R.E. Stevens, W.L. Gladfelter, J. Am. Chem. Soc. 104 (1982) 6454.
[3] R.E. Stevens, R.D. Guettler, W.L. Gladfelter, Inorg. Chem. 29 (1990) 451.
[4] K.K.H. Lee, W.T. Wong, J. Organomet. Chem. 503 (1995) 43.
[5] K.K.H. Lee, W.T. Wong, J. Chem. Soc. Dalton Trans. (1996) 1707.
[6] K.K.H. Lee, W.T. Wong, Inorg. Chem. 35 (1996) 5393.
[7] (a) M.D. Curtis, Inorg. Nucl. Chem. Lett. (1970) 859. (b) R.D. Adams, D.M. Collins, F.A. Cotton, Inorg. Chem. 13 (1974) 1086.
[8] Y. Chi, L.-K. Liu, G. Huttner, L. Zsolnai, J. Organomet. Chem. 390 (1990) 50.
[9] K.A. Kubat-Martin, B. Spencer, L.F. Dahl, Organometallics 6 (1987) 2580.
[10] W. Sun, S. Yang, H. Wang, Y. Yin, K. Yu, Polyhedron 11 (1992) 1143.
[11] D.E. Fjare, D.G. Keyes, W.L. Gladfelter, J. Organomet. Chem. 250 (1983) 383.
[12] (a) H. Beurich, H. Vahrenkamp, Angew. Chem. Int. Ed. Engl. 17 (1978) 863. (b) H. Beurich, H. Vahrenkamp, Chem. Ber. 115 (1982) 2385.
[13] S.-H. Han, J.-S. Song, P.D. Macklin, S.T. Nguyen, G.L. Geoffroy, A.L. Rheingold, Organometallics 8 (1989) 2127.
[14] S. Ermer, K. King, K.I. Hardcastle, E. Rosenberg, A.M.M. Lanfredi, A. Tiripicchio, M.T. Camellini, Inorg. Chem. 22 (1983) 1339.
[15] O. Rossell, M. Seco, G. Segalés, S. Alvarez, M.A. Pellinghelli, A. Tiripicchio, Organometallics 13 (1994) 2205.

[16] J.A. Smieja, R.E. Stevens, D.E. Fjare, W.L. Gladfelter, Inorg. Chem. 24 (1985) 3206.
[17] B.F.G. Johnson, J. Lewis, J.M. Mace, J. Chem. Soc. Chem. Commun. (1984) 186.
[18] M.M. Mickiewicz, C.L. Raston, A.H. White, S.B. Wild, Aust. J. Chem. 30 (1977) 1685.
[19] A.C.T. North, D.C. Phillips, F.S. Mathews, Acta Crystallogr. Sect. A 24 (1968) 351.
[20] D.T. Cromer, J.T. Waber, Internation Tables for X-Ray Crystallography, Kynoch Press, Birmingham, 4 (1974); (a) Table 2.2B; (b) Table 2.3.1.
[21] M.C. Burla, M. Camalli, G. Cascarano, C. Giacovazzo, G. Polidori, R. Spagna, D. Viterbo, J. Appl. Crystallogr. 22 (1989) 389.
[22] TEXSAN, Crystal Structure Analysis Package, Molecular Structure Corporation, 1985 and 1992.